*J. London Math. Soc.* (2) 99 (2019) 807–830 
doi:10.1112/jlms.12195

# Geometry of biperiodic alternating links

Abhijit Champanerkar, Ilya Kofman and Jessica S. Purcell


## Abstract

A biperiodic alternating link has an alternating quotient link in the thickened torus. In this paper, we focus on semi-regular links, a class of biperiodic alternating links whose hyperbolic structure can be immediately determined from a corresponding Euclidean tiling. Consequently, we determine the exact volumes of semi-regular links. We relate their commensurability and arithmeticity to the corresponding tiling, and assuming a conjecture of Milnor, we show there exist infinitely many pairwise incommensurable semi-regular links with the same invariant trace field. We show that only two semi-regular links have totally geodesic checkerboard surfaces; these two links satisfy the Volume Density Conjecture. Finally, we give conditions implying that many additional biperiodic alternating links are hyperbolic and admit a positively oriented, unimodular geometric triangulation. We also provide sharp upper and lower volume bounds for these links.


## 1. *Introduction*

It is well known, due to work of Menasco in the 1980s, that there exists a hyperbolic structure on the complement of any prime alternating link in $S^3$ that is not a $(2, q)$-torus link [26]. The alternating diagram also provides a natural explicit decomposition of the link complement into two ideal *checkerboard polyhedra* with faces identified [6, 25]. Aitchison and Reeves [7] studied alternating links for which these combinatorial polyhedra can be realized directly as ideal hyperbolic polyhedra that can be glued together to obtain the complete hyperbolic structure on the link complement. They called such links *completely realizable*, and they described a large family of completely realizable alternating links, called Archimedean links. Because the geometry of a completely realizable link is explicit, and matches the combinatorics of the polyhedral decomposition, it is easy to determine various geometric properties from its diagram, such as its exact hyperbolic volume. However, there are only finitely many Archimedean links.

There are also a few known infinite families of completely realizable alternating links in $S^3$, built from prisms and antiprisms; these are mentioned in [7], and described in some detail in Thurston's notes [32, Section 6.8]. As far as we are aware, these are the only possibilities for completely realizable alternating links in the 3-sphere.

In this paper we show that, in contrast, there are many infinite families of alternating links in the thickened torus $T^2 \times I$ that are completely realizable, for an analogous notion of a polyhedral decomposition. Moreover, the geometric structure of these links, called semi-regular links, can be immediately determined from a corresponding Euclidean tiling. Thus, geometric invariants, such as hyperbolic volume, arithmeticity and commensurability, can be computed directly from this tiling.

When lifted to the universal cover of $T^2 \times I$, a link $L$ in $T^2 \times I$ becomes a biperiodic link $\mathcal{L}$ in $\mathbb{R}^3$. Conversely, any biperiodic alternating link $\mathcal{L}$ is invariant under translations by a two-dimensional lattice $\Lambda$, such that $L = \mathcal{L}/\Lambda$ is an alternating link in $T^2 \times I$. Thus, equivalently, we prove that infinitely many biperiodic alternating links are completely realizable, and we

Received 27 February 2018; revised 7 November 2018; published online 28 November 2018.

2010 *Mathematics Subject Classification* 57M27, 57M50, 57M25 (primary).

The first two authors acknowledge support by the Simons Foundation and PSC-CUNY. The third author acknowledges support by the Australian Research Council.

determine their geometric properties. Note that the hyperbolic structures of these completely realizable biperiodic alternating links were discovered independently by Adams, Calderon, and Mayer [3].

In addition, for a large class of biperiodic links whose quotient admits a certain kind of alternating diagram on the torus, we find a hyperbolic structure on the complement with a possibly incomplete *geometric triangulation*. That is, the complement decomposes into tetrahedra that are all positively oriented with positive volume. It is still unknown whether or not every link in $S^3$ admits a geometric triangulation. Moreover, we prove that this triangulation is unimodular, and we find sharp lower and upper bounds for the hyperbolic volume. See Theorem 7.5.

The results on complete realizability have a number of interesting consequences:

*Exact volume and cusp shapes.* We compute exact volumes for semi-regular links in terms of their corresponding Euclidean tiling. Their cusp shapes can also be computed from this tiling. See Theorem 3.5 and Corollary 3.10.

*Commensurability and arithmeticity.* Recall that two manifolds are *commensurable* if they admit a common finite sheeted cover. The *trace field* of a hyperbolic manifold $\mathbb{H}^3/\Gamma$ is the smallest field containing the traces of elements, and it is known to be a commensurability invariant of link complements. However, families of links are known to be pairwise incommensurable and yet have the same trace field, for example, [15]. Using the geometry of semi-regular links, we show that this phenomenon also holds for such links. Infinitely many of them have trace field $\mathbb{Q}(i, \sqrt{3})$ but are pairwise incommensurable, assuming a conjecture of Milnor on the Lobachevsky function. Conversely, we also find infinitely many such links that are commensurable to the figure-8 knot complement, and one commensurable to the Whitehead link. See Theorem 4.1.

*Totally geodesic checkerboard surfaces.* It is an open question whether any alternating knot admits two totally geodesic checkerboard surfaces. Only a few links in $S^3$ are known to admit totally geodesic checkerboard surfaces, including the Borromean rings [2]. Pretzel knots $K(p, p, p)$ admit one totally geodesic checkerboard surface, but not two [5]. Our geometric structures allow us to show that two semi-regular links have totally geodesic checkerboard surfaces, namely the infinite square weave and the triaxial link. However, we prove that no other semi-regular alternating links have this property. See Theorem 5.1.

*Volume Density Conjecture.* The volume density of a link in $S^3$ or $T^2 \times I$ is defined to be the ratio of its volume to crossing number. For a biperiodic alternating link, the volume density is that of its quotient link in $T^2 \times I$. In previous work, the authors showed that if a sequence of knots or links in $S^3$ converges in an appropriate sense (see Definition 6.1) to the infinite square weave, then their volume densities approaches the volume density of the infinite square weave [13]. The *Volume Density Conjecture* (Conjecture 6.5) is that the same result holds for any biperiodic alternating link. In this paper, we prove the Volume Density Conjecture for the triaxial link, which has consequences for volume and determinant, as in [10, 12, 13]. See Theorem 6.7.

Elsewhere, biperiodic links have been called *tiling links* [3], *textile links* [9], and *textile structures* [28].

### 1.1. *Organization*

In Section 2, we describe the decomposition of the link complement $(T^2 \times I) - L$. In Section 3, we prove that semi-regular links are completely realizable, and their geometric structure and

hyperbolic volume is determined by the corresponding Euclidean tiling. In Section 4, we relate the geometry of the tiling to the commensurability, arithmeticity, and invariant trace fields of the corresponding semi-regular links. Sections 5 and 6 focus on two special links, namely the square weave and the triaxial link. In Section 5, we prove that these are the only two semi-regular links that have totally geodesic checkerboard surfaces. In Section 6, we prove the Volume Density Conjecture for the triaxial link. Finally, Section 7 is more broad. We prove that if any link $L$ in $T^2 \times I$ admits a certain kind of alternating diagram on the torus, not just semi-regular, then $(T^2 \times I) - L$ is hyperbolic and admits a positively oriented, geometric triangulation. We then find sharp lower and upper bounds for the hyperbolic volume of these links.

## 2. *Torihedra*

Let $I = (-1, 1)$. Let $L$ be a link in $T^2 \times I$ with an alternating diagram on $T^2 \times \{0\}$, projected to the 4-valent graph $G(L)$. First, we eliminate a few simple cases. If $G(L)$ is contained in a disk in $T^2 \times \{0\}$, then the link complement will be reducible, with an essential sphere enclosing a neighborhood of the disk. A similar argument shows that if a complementary region of $G(L)$ is a punctured torus, the link complement is reducible. Hence, we may assume that all complementary regions in $(T^2 \times \{0\}) \setminus G(L)$ are disks or annuli. We will say the diagram is *cellular* if the complementary regions are disks. We call the regions the *faces* of $L$ or of $G(L)$. Similarly, if $\mathcal{L}$ is the biperiodic link with quotient link $L$, then the faces of $\mathcal{L}$ refer to the complementary regions of its diagram in $\mathbb{R}^2$, which are the regions $\mathbb{R}^2 - G(\mathcal{L})$. We will say the diagram of $L$ on $T^2 \times \{0\}$ is *reduced* if four distinct faces meet at every crossing of $G(\mathcal{L})$ in $\mathbb{R}^2$. Note that a reduced cellular diagram has at least one crossing in $T^2 \times \{0\}$, and an alternating, reduced, cellular diagram has at least two crossings. Throughout the paper, we will work with diagrams on $T^2 \times \{0\}$ that are alternating, reduced, and cellular.

Definition 2.1. A *torihedron* is a cone on the torus, that is, $T^2 \times [0, 1]/(T^2 \times \{1\})$, with a cellular graph $G$ on $T^2 \times \{0\}$. An *ideal torihedron* is a torihedron with the vertices of $G$ and the vertex $T^2 \times \{1\}$ removed. Hence, an ideal torihedron is homeomorphic to $T^2 \times [0, 1)$ with a finite set of points (ideal vertices) removed from $T^2 \times \{0\}$.

Let $M = (T^2 \times I) - L$ be the link complement. The checkerboard polyhedral decomposition of the complement of an alternating link in $S^3$, as in [6, 25], can be generalized to that of an alternating link in $T^2 \times I$. This was done for a single example in [13], and much more generally in [22]. The following version is appropriate for the links considered here:

Theorem 2.2. *Let $L$ be a link in $T^2 \times (-1, 1)$ with a reduced, cellular, alternating diagram on $T^2 \times \{0\}$. Then the link complement $M = (T^2 \times I) - L$ admits a decomposition into two ideal torihedra $M_1$ and $M_2$ with the following properties.*

(1) *$M_1$ is homeomorphic to $T^2 \times [0, 1)$ and $M_2$ is homeomorphic to $T^2 \times (-1, 0]$, each with finitely many vertices removed from $T^2 \times \{0\}$. The points $T^2 \times \{\pm 1\}$ are ideal vertices denoted by $\pm\infty$.*
(2) *$T^2 \times \{0\}$ on $M_1$ and $M_2$ is labeled with the diagram graph $G(L)$, with vertices removed. Thus, the graph has 4-valent ideal vertices.*
(3) *$M$ is obtained by gluing $M_1$ to $M_2$ along their faces on $T^2 \times \{0\}$. Faces of $G(L)$ are checkerboard colored, and glued via a homeomorphism that rotates the boundary of each face by one edge in a clockwise or anti-clockwise direction, depending on whether the face is white or shaded.*

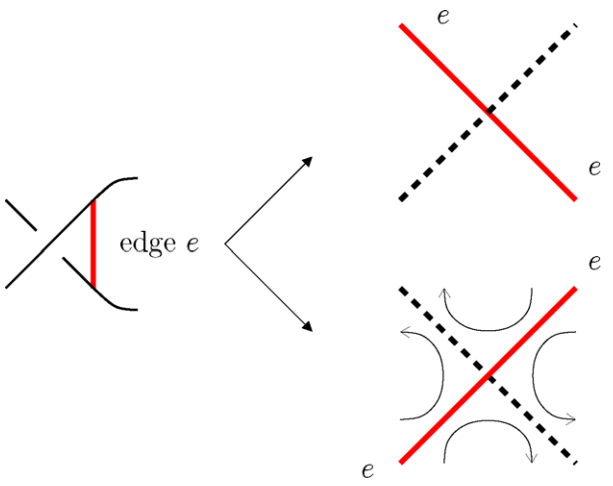


FIGURE 1 (colour online). *Crossing edge $e$ at a 4-valent vertex, and corresponding copies of $e$ on the upper and lower torihedra. The arrows on the lower diagram indicate the direction of twisting for gluing faces.*

(4) *Each edge class contains exactly four edges, and these edges are the crossing arcs of the link complement. At each ideal vertex, a pair of opposite edges are identified, in both $M_1$ and $M_2$, with the opposite pair identified at the same vertex in $M_1$ and $M_2$. See Figure 1.*

We will refer to $M_1$ and $M_2$ as the upper and lower torihedra of $L$. When there is no ambiguity, the torihedron will be denoted by $P(L)$.

*Proof of Theorem* 2.2. We proceed exactly as in [**25**], but instead of two 3-balls, we start with a decomposition of $T^2 \times I$ into two thickened tori $T^2 \times [0, 1)$ and $T^2 \times (-1, 0]$. The torihedra are formed by cutting along checkerboard surfaces; an arc of intersection between such surfaces becomes an ideal edge of the decomposition. The form of the torihedra near a crossing is illustrated in Figure 1. Since $L$ has an alternating, reduced, and cellular diagram, the 1-skeleton of each torihedron is the same as $G(L)$, and its vertices are ideal (removed). The remainder of the construction for the cell decompostion and the face identification in [**25**] is completely local at every crossing, and hence goes through likewise in the toroidal case. □

These decompositions can be extended to biperiodic alternating links.

THEOREM 2.3. *Let $\mathcal{L}$ be a biperiodic alternating link whose quotient link $L$ in $T^2 \times I$ has a reduced, cellular, alternating diagram on $T^2 \times \{0\}$. Then, $\mathbb{R}^3 - \mathcal{L}$ admits a decomposition into two identical infinite ideal polyhedra. Each infinite polyhedron $P(\mathcal{L})$ is homeomorphic to $\mathbb{R}^2 \times [0, \infty)$, with a biperiodic planar graph identical to $G(\mathcal{L})$ in $\mathbb{R}^2 \times 0$ with vertices removed. The polyhedra are glued via a homeomorphism determined by the checkerboard coloring of faces of $G(\mathcal{L})$ as in Theorem 2.2.*

*Proof.* Lift the torihedral decomposition of Theorem 2.2 to the cover $\mathbb{R}^3 - \mathcal{L}$ of $(T^2 \times I) - L$. □

### 2.1. *Geometric torihedra and stellation*

We now wish to determine conditions that guarantee the torihedra admit a hyperbolic structure. In [**22**], it was shown that if such a link on $T^2 \times I$ is weakly prime (see Definition 7.1),

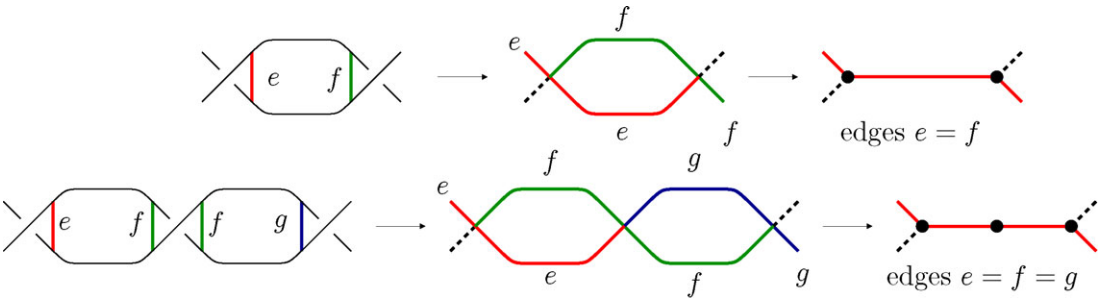


FIGURE 2 (colour online). *Top: Collapsing a bigon creates an edge with* 3*-valent endpoints. Bottom: Collapsing a sequence of bigons creates a chain of edges with* 3*-valent end vertices.*

then the link complement is hyperbolic. However, the torihedra themselves may not admit a hyperbolic structure. For example, if $G(\mathcal{L})$ or, equivalently, $G(L)$ has bigon faces, there is no way the torihedra and polyhedra as constructed can admit a hyperbolic structure. While geometric information can be obtained even if the torihedra are not hyperbolic, we will obtain much stronger results when they are. Thus, we will modify the torihedra by collapsing bigons.

DEFINITION 2.4. Let $\mathcal{L}$ be a biperiodic alternating link whose quotient link $L$ in $T^2 \times I$ has a reduced, cellular, alternating diagram on $T^2 \times \{0\}$. We define the graph $T_L$ on $T^2 \times \{0\}$ by collapsing all bigons of the diagram graph $G(L)$, as shown in Figure 2. If $L$ has no bigons, then $T_L = G(L)$. By lifting to the cover, we obtain a graph denoted $T_{\mathcal{L}}$ on $\mathbb{R}^2 \times \{0\} \subset \mathbb{R}^3$ by collapsing all bigons of $G(\mathcal{L})$.

LEMMA 2.5. *Let $L$ be a link in $T^2 \times I$ with a reduced, cellular, alternating diagram on $T^2 \times \{0\}$. Let $M_1$ and $M_2$ be the torihedra in Theorem 2.2. Collapse each bigon in $M_1$ and $M_2$. Then, $M = (T^2 \times I) - L$ has a decomposition into ideal torihedra with the following properties.*

(1) *$T^2 \times \{0\}$ on $M_1$ and $M_2$ contains a graph $T_L$ as in Definition 2.4 with its vertices removed. Thus, the valences of ideal vertices are* 4, 3, *and* 2, *depending on whether the corresponding vertex of $G(L)$ is adjacent to* 0, 1, *or* 2 *bigons.*

(2) *$M$ is obtained by gluing faces on $M_2$ to faces on $M_1$ by a homeomorphism that rotates the boundary of each face by a single rotation in one edge, clockwise or anti-clockwise depending on whether the same face in $G(L)$ is white or shaded.*

(3) *Each edge class corresponds to a crossing arc as before, but crossing arcs associated to crossings adjacent across a bigon are identified into a single edge. Thus, if a crossing is adjacent to no bigons, the corresponding edge has degree* 4. *If it is adjacent to a twist region with $n$ bigons, the corresponding edge has degree $4 + 2n$.*

*By lifting to the cover, a similar decomposition holds for $\mathbb{R}^3 - \mathcal{L}$, with the graph $T_{\mathcal{L}}$ on $\mathbb{R}^2 \times \{0\} \subset \mathbb{R}^3$.*

*Proof.* The proof is by tracing the result of collapsing a bigon in torihedra $M_1$ and $M_2$, similar to the process for collapsing bigons in the polyhedral decomposition of an alternating link in $S^3$. This is illustrated in Figure 2. □

We now turn the torihedral decomposition into a triangulation.

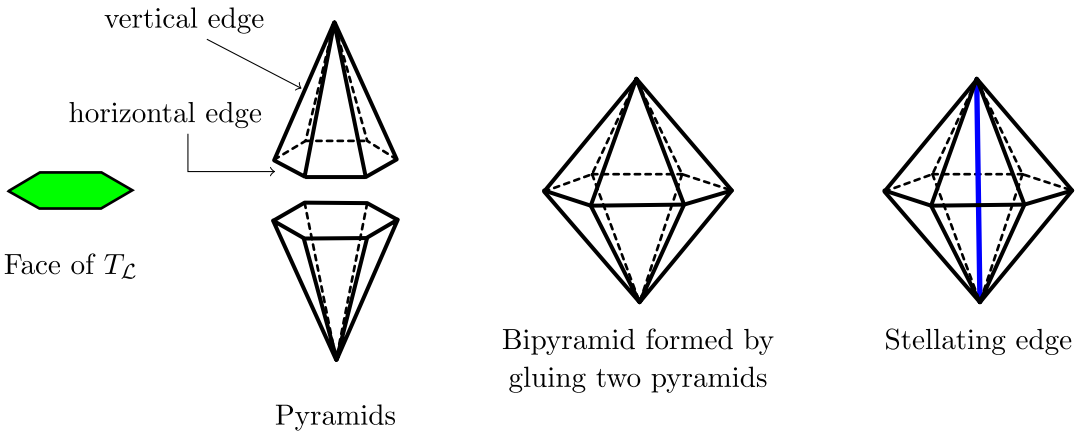


FIGURE 3 (colour online). *Horizontal, vertical, and stellating edges of the stellated bipyramid triangulation.*

LEMMA 2.6. *Let $L$ be a link in $T^2 \times I$ with a reduced, cellular, alternating diagram on $T^2 \times \{0\}$. Then, the link complement $M = (T^2 \times I) - L$ admits a decomposition into ideal tetrahedra with the following properties.*

(1) *Edges are labeled as horizontal, vertical, and stellating. Each horizontal edge corresponds to an edge of $T_L$, and is identified to other horizontal edges. Each vertical edge runs from an ideal vertex of $M_1$ or $M_2$ to $\pm\infty$. Each stellating edge runs through the center of a non-triangular face in the complement of $T_L$, from $-\infty$ to $+\infty$.*
(2) *For $n \geqslant 3$, each $n$-gon region in the complement of $T_L$ on $T^2 \times \{0\}$ is divided into $n$ ideal tetrahedra.*

Denote the collection of ideal tetrahedra of Lemma 2.6 by $\mathcal{T}$. We will call $\mathcal{T}$ the *stellated bipyramid triangulation.*

*Proof.* Cone each face of $T_L$ on $T^2 \times \{0\}$ to $\pm\infty$, respectively, obtaining a bipyramid. Edges of the pyramids that are incident to $\pm\infty$ become *vertical edges*. Edges of the pyramids that are edges of $T_L$ become *horizontal edges*. See Figure 3.
Now, for each face of $T_L$, glue the upper pyramid on that face to the lower pyramid according to the checkerboard coloring, as described in Lemma 2.5. This provides a decomposition of $(T^2 \times I) - L$ into bipyramids on the faces of $T_L$. Obtain an ideal triangulation $\mathcal{T}$ of $(T^2 \times I) - L$ by stellating the bipyramids into tetrahedra by adding *stellating edges*, as shown in Figure 3. □

By taking the cover of $(T^2 \times I) - L$, Lemma 2.6 gives a decomposition of $\mathbb{R}^3 - \mathcal{L}$ into ideal tetrahedra. This decomposition was used in [**13**] to triangulate the infinite square weave. It was extended to alternating links in $S^3$ in [**4**] and to links in thickened higher genus surfaces in [**3**]. Our work here for links in $T^2 \times I$ was done independently.

## 3. *Semi-regular alternating links*

In this section, we study a class of biperiodic alternating links whose geometric structure and hyperbolic volume can be immediately determined from a corresponding Euclidean tiling. For

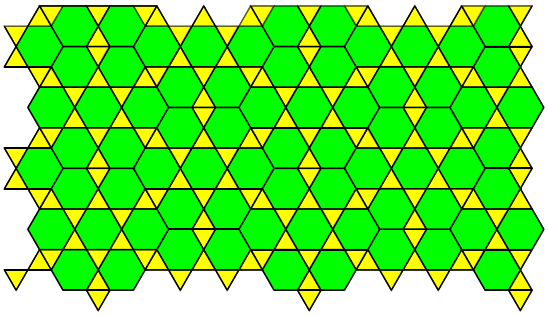

FIGURE 4 (colour online). *A tiling with isolated* 3*-valent vertices. Figure modified from* [**33**].

the tilings considered in this section, the vertices can only be 3-valent or 4-valent; that is, the links $L$ or $\mathcal{L}$ can have at most one bigon per twist region.

DEFINITION 3.1. A biperiodic alternating link $\mathcal{L}$ is called *semi-regular* if $T_{\mathcal{L}}$ is isomorphic, as a plane graph, to a biperiodic edge-to-edge Euclidean tiling with convex regular polygons. We also say the quotient link $L$ is *semi-regular*, and refer to the quotient tiling of $T^2$ as $T_L$.

Note that a semi-regular link is reduced and cellular.

If the link has no bigons, then $T_{\mathcal{L}}$ is isomorphic to $G(\mathcal{L})$. Since there is at most one bigon in every twist region of $\mathcal{L}$, for every bigon, both endpoints of the corresponding edge in $T_{\mathcal{L}}$ are 3-valent. Thus, if $V_4(T_{\mathcal{L}})$ denotes the subset of 4-valent vertices, then the graph $T_{\mathcal{L}} - V_4(T_{\mathcal{L}})$ admits a perfect matching, defined as follows.

DEFINITION 3.2. A *perfect matching* on a graph is a pairing of adjacent vertices that includes every vertex exactly once.

Figure 4 shows an example of a tiling with isolated 3-valent vertices. Hence, this tiling cannot be associated with a semi-regular biperiodic alternating link.

We now discuss local shapes for Euclidean tilings with 3- and 4-valent vertices. Let $T$ be a biperiodic edge-to-edge Euclidean tiling with convex regular polygons. Grünbaum and Shephard [**20**] classified such tilings according to the pattern of polygons at each vertex. They described 21 vertex types which can occur in $T$. If an $a$–gon, $b$–gon, $c$–gon, etc. appear in cyclic order around the vertex, then its type is denoted by $a.b.c\ldots$. For example, the square tiling has vertex type 4.4.4.4.

LEMMA 3.3. *Let $T$ be any biperiodic edge-to-edge Euclidean tiling with convex regular polygons, with vertices of valence* 3 *and* 4*, such that $T - V_4(T)$ admits a perfect matching.*

(i) *If $T$ has only* 4*-valent vertices, then the only polygons that can occur in $T$ are triangles, squares, and hexagons, and every vertex of $T$ has one of five vertex types:*

$$3.3.6.6, \quad 3.6.3.6, \quad 3.4.4.6, \quad 3.4.6.4, \text{ or } 4.4.4.4$$

(ii) *If $T$ has only* 4*-valent vertices, the number of triangles is twice the number of hexagons in the fundamental domain.*

(iii) *If $T$ has* 3*-valent vertices, then the only polygons that can occur in $T$ are triangles, squares, hexagons, octagons, and dodecagons.*

The allowable vertex types for part (i) are shown in Figure 5.

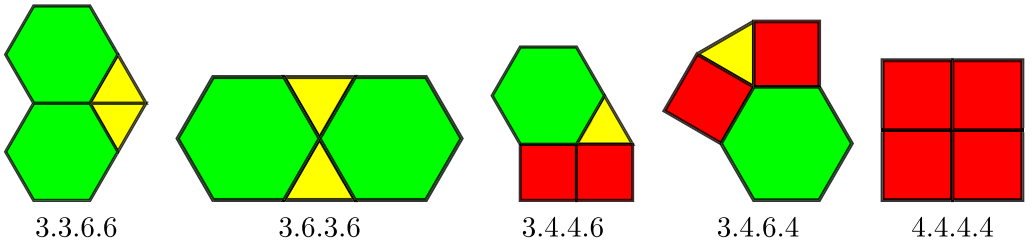


FIGURE 5 (colour online). *Allowable vertex types for tilings with only* 4*-valent vertices.*

*Proof.* Part (i): Among the 21 vertex types classified in [20], there are only seven 4-valent vertex types. These are the five types discussed above, plus two more types that include a dodecagon: 3.4.3.12 and 3.3.4.12. But allowing only these seven types of 4-valent vertices makes it impossible to extend a tiling from a vertex of the dodecagon to a tiling of the whole plane. A straightforward case-by-case analysis shows that if a dodecagon is present, then all the vertices of the dodecagon cannot be of type 3.4.3.12 or 3.3.4.12, thus ruling out a dodecagon among the vertex types for a 4-valent tiling.

Part (ii): If $t, s, h$ are the numbers of triangles, squares, and hexagons, respectively, in the fundamental domain, then we have $4v = 2e = 6h + 4s + 3t$ and $f = h + s + t$. Now, since the fundamental domain gives a tiling of the torus, $v - e + f = 0$ which implies that $t = 2h$.

Part (iii): Again we consider the 21 vertex types classified in [20]. Ten of these give a 3-valent vertex, and those of type 4.8.8, 6.6.6, 3.12.12, and 4.6.12 satisfy the conditions of the lemma. We show that the others cannot appear. For each of the other types, all but 5.5.10 contain an $n$-gon that appears in no other vertex types, namely $n = 15$, 18, 20, 24, and 42. In each of these cases, since we allow only 3- and 4-valent vertices, each of the vertices meeting the $n$-gon must be of the same vertex type, namely the unique 3-valent vertex meeting that $n$-gon. But now we step through each case and check that no tiling of the plane exists with these vertices on the $n$-gon, and only 3- and 4-valent vertex types away from the $n$-gon. Finally, once we have ruled out the other types, the same argument applies for the case 5.5.10: all vertices must be of type 5.5.10, and we cannot complete the tiling. □

THEOREM 3.4. *Every biperiodic edge-to-edge Euclidean tiling $T$ with convex regular polygons, with vertices of valence* 3 *or* 4*, such that $T - V_4(T)$ admits a perfect matching, is the tiling $T_{\mathcal{L}}$ for a semi-regular biperiodic link $\mathcal{L}$.*

*Proof.* Given a tiling, note that if all vertices of $T$ are 4-valent, then $T = G(\mathcal{L}) = T_{\mathcal{L}}$ for a semi-regular link $\mathcal{L}$ with no bigons simply by replacing vertices with crossings in an alternating manner. Otherwise, if the tiling $T$ has 3-valent vertices, then the perfect matching condition implies that the 3-valent vertices of $T$ can be covered by a subset of mutually disjoint edges. We double each of these edges to obtain the projection $G(\mathcal{L})$ of a semi-regular link $\mathcal{L}$ with bigons. Then, the graph $T_{\mathcal{L}}$ of Lemma 2.5 is exactly $T$. □

Let $v_{\text{tet}} \approx 1.01494$ and $v_{\text{oct}} \approx 3.66386$ be the hyperbolic volumes of the regular ideal tetrahedron and the regular ideal octahedron, respectively. Also let $v_{16} \approx 7.8549$ and $v_{24} \approx 10.3725$ denote the volume of a hyperbolic ideal bipyramid over a regular octagon and regular dodecagon, respectively, with 16 and 24 faces.

The main result in this section is the following theorem. Part (1) was proved independently in [3].

THEOREM 3.5. *Let $\mathcal{L}$ be any semi-regular biperiodic link, with alternating quotient link $L$ in $T^2 \times I$, and $T_L$ as in Definition 2.4. Then,*

(1) *$(T^2 \times I) - L$ has a complete hyperbolic structure coming from a decomposition into regular ideal bipyramids on the faces of $T_L$:*
(2) *if $T_L$ is 4–valent, then the volume of $(T^2 \times I) - L$, denoted $\mathrm{vol}(L)$, satisfies*

$$\mathrm{vol}(L) = 10H\, v_{\mathrm{tet}} + S\, v_{\mathrm{oct}},$$

*where the fundamental domain of $\mathcal{L}$ contains $H$ hexagons and $S$ squares:*
(3) *if $T_L$ also has 3-valent vertices, then*

$$\mathrm{vol}(L) = (6H + 2T)\, v_{\mathrm{tet}} + S\, v_{\mathrm{oct}} + \Omega\, v_{16} + D\, v_{24},$$

*where $H$, $T$, $S$, $\Omega$, and $D$ denote the number of hexagons, triangles, squares, octagons, and dodecagons, respectively, in the fundamental domain of $\mathcal{L}$.*

The proof of the theorem uses angle structures.

DEFINITION 3.6. Given an ideal triangulation $\{\Delta_i\}$ of a 3-manifold, an *angle structure* is a choice of three angles $(x_i, y_i, z_i) \in (0, \pi)^3$ for each tetrahedron $\Delta_i$, assigned to three edges of $\Delta_i$ meeting in a vertex, such that

(1) $x_i + y_i + z_i = \pi$;
(2) opposite edges in each $\Delta_i$ are assigned the same angle;
(3) for every edge in the triangulation, the angle sum about the edge is $2\pi$.

Associated to any angle structure is a volume, obtained by summing the volumes of hyperbolic ideal tetrahedra realizing the specified angles. This defines a volume functional over the space of angle structures for a given ideal triangulation of a manifold. The volume functional is convex, and thus has a maximum. If the maximum of the volume functional occurs in the interior of the space of angle structures, then it follows from work of Casson and Rivin that the angle structures at the maximum give the unique complete, finite volume hyperbolic structure on the manifold [**31**] (see also [**19**]). We will prove Theorem 3.5 by finding the unique maximum in the interior of the space of angle structures.

We now slightly modify the stellated bipyramid triangulation $\mathcal{T}$ from Lemma 2.6 by performing a 3-2 move on every stellated bipyramid over a triangular face. As a result, every triangle of $T_{\mathcal{L}}$ corresponds to two ideal tetrahedra, one above and one below the triangular face. Let $\mathcal{T}'$ denote this modified triangulation.

LEMMA 3.7. *Let $L$ be a semi-regular link with no bigons. Then the triangulation $\mathcal{T}'$ of $(T^2 \times I) - L$ admits an angle structure with the following properties.*

(1) *The tetrahedra coming from stellated hexagons are all regular ideal tetrahedra.*
(2) *The tetrahedra coming from each stellated octahedron glue to form a regular ideal octahedron.*
(3) *The tetrahedra above and below every triangular face of $T_L$ are regular ideal tetrahedra.*

*Proof.* Since $L$ has no bigons, $G(L)$ is isomorphic to $T_L$. Recall that all tetrahedra of $\mathcal{T}$ come from stellating bipyramids over all faces of $T_L$, including the triangular faces. We first assign angles to vertical edges. Each vertical edge of the triangulation runs from a vertex of $G(L)$ to $\pm\infty$. The vertex is also a vertex of $T_L$, a Euclidean tiling. The four faces adjacent to this vertex have four interior angles coming from the Euclidean tiling. There are eight tetrahedra

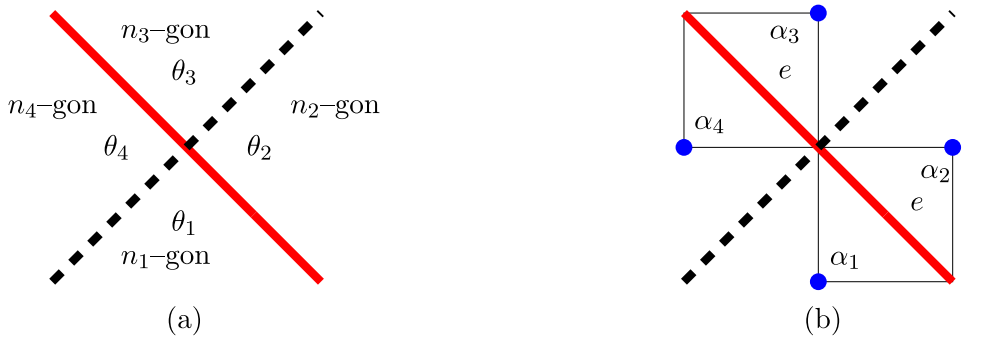


FIGURE 6 (colour online). (a) *Vertex angles $\theta_i$ at a 4-valent vertex of the tiling $T_L$.* (b) *Dihedral angles $\alpha_i = 2\pi/n_i$ at stellating edges of $\mathcal{T}$.*

coming from the stellation adjacent to this vertical edge: two tetrahedra per face adjacent to that vertex in $T_L$. For each tetrahedron, assign to its vertical edge half of the Euclidean interior angle from $T_L$ of the associated face. Because $T_L$ is a Euclidean tiling, it immediately follows that the angle sum around every vertical edge is $2\pi$.

In addition, we obtain further information about adjacent faces. A regular Euclidean $n$-gon has interior angle $(n-2)\pi/n$. If the faces adjacent to a vertex of $T_L$ are an $n_1$-gon, an $n_2$-gon, an $n_3$-gon, and an $n_4$-gon, with interior angles $\theta_1$, $\theta_2$, $\theta_3$, and $\theta_4$, respectively, then the sum of the interior angles at that vertex satisfies

$$\sum_{i=1}^{4} \theta_i = \sum_{i=1}^{4} \frac{(n_i - 2)\pi}{n_i} = 2\pi \Longrightarrow \frac{1}{n_1} + \frac{1}{n_2} + \frac{1}{n_3} + \frac{1}{n_4} = 1. \tag{3.1}$$

See Figure 6(a).

Next we assign angles to the stellating edges. These run from $-\infty$ to $+\infty$ through the center of an $n$-gon face, and are adjacent to $n$ tetrahedra. As the faces of $T_L$ are regular Euclidean polygons, we assign each edge meeting the stellating edge an angle $2\pi/n$, so the angle sum around stellating edges is $2\pi$. Because opposite dihedral angles on each tetrahedron are equal, this also assigns angles to horizontal edges: each has angle $2\pi/n$.

Now consider the angle sum over all angles assigned to edges identified to a fixed horizontal edge $e$. There are exactly four tetrahedra incident to $e$, shown in Figure 6(b), with one tetrahedron in each of the four faces adjacent to a vertex of $T_L$. The dihedral angle on the horizontal edge coming from the $i$th tetrahedron is $\alpha_i = 2\pi/n_i$. Thus, the angle sum at $e$ is

$$\frac{2\pi}{n_1} + \frac{2\pi}{n_2} + \frac{2\pi}{n_3} + \frac{2\pi}{n_4} = 2\pi,$$

where the equality follows by equation (3.1). Therefore, the angles assigned to the horizontal, vertical, and stellating edges make the angle sum $2\pi$ on every edge of $\mathcal{T}$, which gives an angle structure.

Finally, we use this angle structure to get an angle structure on $\mathcal{T}'$. Stellated bipyramids over a triangular face consist of three tetrahedra, each with angle $2\pi/3$ on their horizontal and stellating edges, and angle $\pi/6$ on vertical edges. Replacing these three tetrahedra via a 3-2 move, the stellating edge is removed. At vertical edges, two faces glue to one, so the angle becomes $\pi/3$. At horizontal edges, the angle is halved, becoming $\pi/3$. This results in two ideal tetrahedra with all angles $\pi/3$, which are regular ideal tetrahedra. □

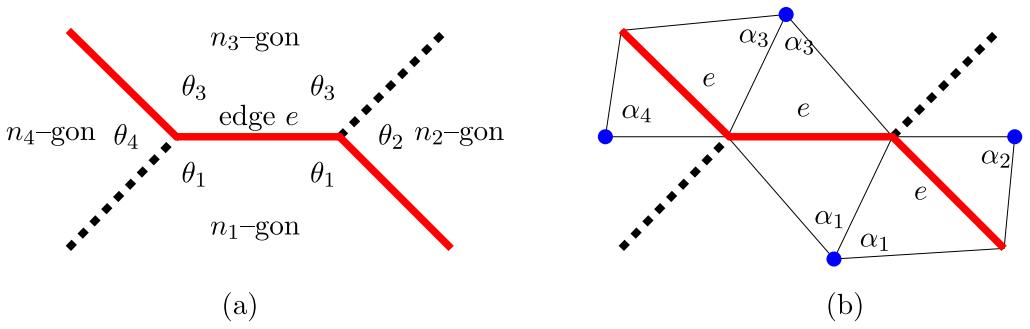


FIGURE 7 (colour online). (a) *Vertex angles $\theta_i$ at a pair of 3-valent vertices of the tiling $T_L$.* (b) *Dihedral angles $\alpha_i = 2\pi/n_i$, $1 \leqslant i \leqslant 4$, at stellating edges of $\mathcal{T}$.*

LEMMA 3.8. *Let $L$ be a semi-regular link with at most one bigon per twist region. Then, the triangulation $\mathcal{T}'$ of $(T^2 \times I) - L$ admits an angle structure with the properties of Lemma 3.7, and additionally*

(4) *tetrahedra coming from octagons glue to form a bipyramid over a regular ideal octagon, and those coming from dodecagons form a bipyramid over a regular ideal dodecagon.*

*Proof.* As in Lemma 3.7, we stellate bipyramids, and assign angles to vertical edges of tetrahedra using the vertex angles of the Euclidean tiling $T_L$. To stellating edges, hence also to horizontal edges, assign angles $2\pi/n$. Again, we need to check that the angle sum around each edge class is $2\pi$. For vertical and stellating edges, and for horizontal edges with no 3-valent endpoints, the proof of Lemma 3.7 applies as before to give angle sum $2\pi$ as desired.

Consider a horizontal edge $e$ with 3-valent endpoints. Recall the effect of collapsing bigons, as in Lemma 2.5: the horizontal edge $e$ will be identified to the crossing arcs of a bigon face, as shown in Figure 2 (top). There are four faces surrounding the two 3-valent vertices of $e$: an $n_1$–gon, an $n_2$–gon, an $n_3$-gon, and an $n_4$-gon, as illustrated in Figure 7(a).

The vertex angle of each regular Euclidean $n_i$-gon is $\theta_i = \frac{(n_i-2)\pi}{n_i}$ for $1 \leqslant i \leqslant 4$. Hence, the following equations express the angle sum around the two endpoints of edge $e$:

$$\frac{(n_1-2)\pi}{n_1} + \frac{(n_2-2)\pi}{n_2} + \frac{(n_3-2)\pi}{n_3} = 2\pi \Longrightarrow \frac{2}{n_1} + \frac{2}{n_2} + \frac{2}{n_3} = 1;$$

$$\frac{(n_1-2)\pi}{n_1} + \frac{(n_3-2)\pi}{n_3} + \frac{(n_4-2)\pi}{n_4} = 2\pi \Longrightarrow \frac{2}{n_1} + \frac{2}{n_3} + \frac{2}{n_4} = 1.$$

Adding the equations on the right, we obtain:

$$\frac{2}{n_1} + \frac{1}{n_2} + \frac{2}{n_3} + \frac{1}{n_4} = 1. \tag{3.2}$$

Now, the horizontal edge $e$ associated to the crossing arc of a bigon is identified to six tetrahedra, as shown in Figure 7(b). The angle sum at edge $e$ is

$$\frac{4\pi}{n_1} + \frac{2\pi}{n_2} + \frac{4\pi}{n_3} + \frac{2\pi}{n_4} = 2\pi,$$

where the equality follows by equation (3.2). Thus, this angle assignment gives the desired angle structure.

To complete the proof, perform a 3-2 move on the stellated bipyramids over triangles, as in the proof of Lemma 3.7. As before, we obtain two regular ideal tetrahedra for each triangular face of $T_L$. □

LEMMA 3.9. *Let $L$ be a semi-regular link. For the triangulation $\mathcal{T}'$ of $(T^2 \times I) - L$, let $\mathcal{A}(\mathcal{T}')$ be the set of angle structures on $\mathcal{T}'$. Then, the volume functional* $\mathrm{vol}\colon \mathcal{A}(\mathcal{T}') \to \mathbb{R}$ *is maximized at the angle structure of Lemma 3.7 or Lemma 3.8, depending on whether or not $T_L$ has 3-valent vertices.*

*Proof.* If $L$ has no bigons, then by Lemma 3.3($i$), the only regular $n$-gons that can arise in $T_L$ have $n = 3$, 4, or 6. If $L$ has bigons, then 3-valent vertices appear in pairs, and octagons and dodecagons can also arise.

The tetrahedra coming from regular triangles and hexagons have the angles of a regular ideal tetrahedron. Since the volume of a tetrahedron is maximized by the regular ideal tetrahedron, the given angle structure maximizes the volume of these tetrahedra.

For $n = 4$, 8, or 12, we claim that the tetrahedra obtained by stellating the regular 4, 8, and 12-bipyramids also maximize volume. The regular 4-bipyramid is the regular ideal octahedron, which has volume $v_{\mathrm{oct}}$. If we combine the tetrahedra obtained by stellating the square bipyramids, we obtain a decomposition of $(T^2 \times I) - L$ into regular tetrahedra and octahedra. In [**14**, Lemma 3.3], we proved that for any angle structure on an ideal octahedron $P$, the volume of that angle structure satisfies $\mathrm{vol}(P) \leqslant v_{\mathrm{oct}}$. The same argument applies as well for $n = 8$ and $n = 12$: by work of Rivin [**31**], an angle structure will have volume bounded by the unique complete hyperbolic structure on the $n$-bipyramid with that angle assignment. But the maximal volume of a complete ideal $n$-bipyramid is obtained uniquely by the regular $n$-bipyramid (see [**1**, Theorem 2.1]).

Therefore, whether or not $L$ has bigons, the angle structure on $\mathcal{T}'$ maximizes volume. □

*Proof of Theorem* 3.5. In Lemmas 3.7 and 3.8, we found an angle structure on an ideal triangulation of the complement of any semi-regular biperiodic link, and by Lemma 3.9, that angle structure maximizes volume. Work of Casson and Rivin implies that the gluing of hyperbolic ideal tetrahedra that realize this angle structure gives the complete finite volume structure on $(T^2 \times I) - L$. This completes the proof of part (1).

To prove parts (2) and (3), it remains to apply Lemma 3.3, describing which Euclidean tilings can occur as $T_{\mathcal{L}}$. For part (2), by Lemma 3.3(ii), there are twice the number of triangles as hexagons. A bipyramid on a regular hexagon decomposes into six regular ideal tetrahedra, which contribute $6v_{\mathrm{tet}}$ to the volume. Since every triangle contributes two regular ideal tetrahedra, it follows that every hexagon contributes $10v_{\mathrm{tet}}$ to the volume. Thus, if $T_{\mathcal{L}}$ has $H$ hexagons and $S$ squares per fundamental domain, then the volume density of $\mathcal{L}$ is $10H\, v_{\mathrm{tet}} + S\, v_{\mathrm{oct}}$ per fundamental domain.

Similarly for part (3), for each regular $n$–gon face of $T_{\mathcal{L}}$, the contribution to the volume is that of a regular $n$–bipyramid. This proves the result. □

COROLLARY 3.10. *Let $\mathcal{L}$ be any semi-regular biperiodic link, with alternating quotient link $L$ in $T^2 \times I$. Then the cusps of $(T^2 \times I) - L$ satisfy the following.*

(1) *Cusps corresponding to $T^2 \times \{\pm 1\}$ have fundamental domain identical to a fundamental domain of the corresponding Euclidean tiling $T_{\mathcal{L}}$.*

(2) *Cusps corresponding to components of $L$ are tiled by regular triangles and squares in the case $L$ has no bigons, and otherwise by regular triangles and squares, and triangles obtained by stellating a regular octagon and a regular dodecagon.*

*Proof.* The second item follows from the fact that $(T^2 \times I) - L$ is obtained by gluing regular tetrahedra and octahedra, and the tetrahedra obtained by stellating bipyramids over regular octagons and dodecagons in the case of bigons. The first follows from the fact that the pattern of such polygons meeting the cusps corresponding to $T^2 \times \{\pm 1\}$ comes from the Euclidean tiling. □

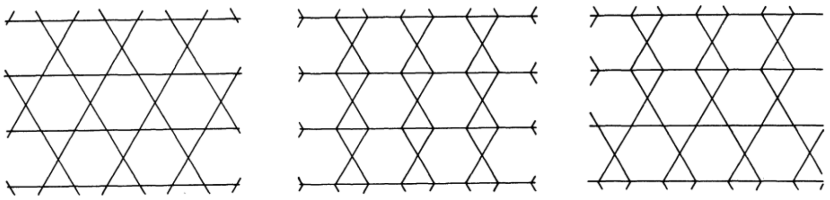

FIGURE 8. *Figure 4 from* [**20**] *showing three of the infinitely many semi-regular links with triangles and hexagons.*

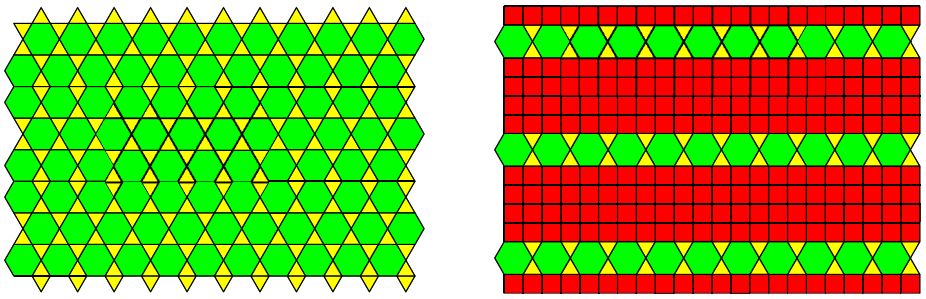

FIGURE 9 (colour online). *Left: Tiling for one of the infinitely many semi-regular links commensurable with the figure-8 knot. Right: Tiling for $\mathcal{L}_2$, one of a pairwise incommensurable family of semi-regular links $\mathcal{L}_i$ with the same invariant trace field. Figures modified from* [**33**].

## 4. *Commensurability and arithmeticity of semi-regular links*

The proof of Theorem 3.5 enables us to compute the invariant trace fields of semi-regular links without bigons. In Theorem 4.1 below, we relate the geometry of the tiling to the commensurability, arithmeticity and invariant trace fields of the corresponding links. Milnor [**27**] conjectured that, except for certain well-known relations, values of the Lobachevsky function at rational multiples of $\pi$ are rationally independent. In particular, its values at $\pi/3$ and $\pi/4$ are conjectured to be rationally independent. Assuming this, we show that there exist infinitely many semi-regular links that are pairwise incommensurable, but have the same invariant trace field.

THEOREM 4.1. *For a semi-regular link $\mathcal{L}$ with no bigons, with alternating quotient link $L$, let $M = (T^2 \times I) - L$ and let $k(M)$ denote its invariant trace field.*

(1) *If the fundamental domain of $T_{\mathcal{L}}$ contains only squares, then $k(M) = \mathbb{Q}(i)$, and $M$ is commensurable to the Whitehead link complement. Hence, $M$ is arithmetic. In this case, $\mathcal{L}$ is the unique semi-regular link called the square weave $\mathcal{W}$ below.*

(2) *If the fundamental domain of $T_{\mathcal{L}}$ contains only triangles and hexagons, then $k(M) = \mathbb{Q}(i\sqrt{3})$, and $M$ is commensurable to the figure-8 knot complement. Hence, $M$ is arithmetic. In this case, $\mathcal{L}$ is one of infinitely many semi-regular links. Examples are shown in Figures 8 and 9 (left).*

(3) *If the fundamental domain of $T_{\mathcal{L}}$ contains at least one hexagon and one square, then $k(M) = \mathbb{Q}(i, \sqrt{3})$. Hence, $M$ is not arithmetic. Assuming $v_{\text{tet}}$ and $v_{\text{oct}}$ are rationally independent, there are infinitely many commensurability classes of semi-regular links with this invariant trace field (for example, see Figure 9 (right)).*

*Proof.* We first compute the invariant trace fields in all the three cases. Another way of looking at the proof of Theorem 3.5 (1) is that the edge gluing equations for $\mathcal{T}'$ have solutions

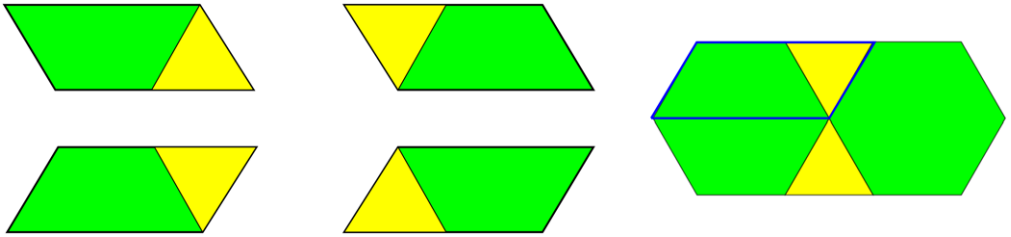

FIGURE 10 (colour online). *Left: Four parallelograms which comprise strips of the tiles* 3.6.3.6 *and* 3.3.6.6. *Right: One of the parallelograms fitting on the tile* 3.6.3.6.

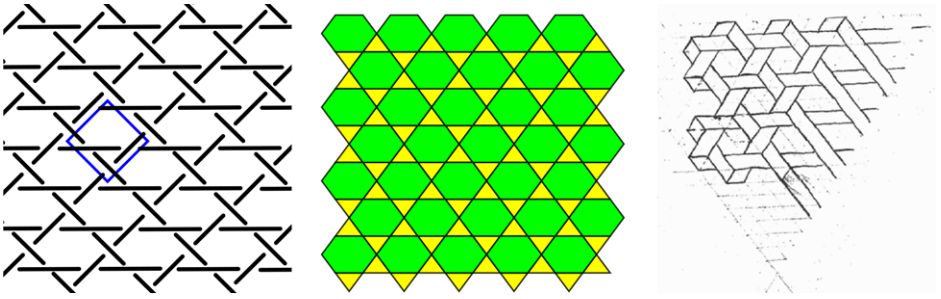

FIGURE 11 (colour online). *Left to right: Triaxial link* $\mathcal{L}$ *with a fundamental domain (blue square), trihexagonal tiling* $T_{\mathcal{L}}$*, and a figure from Gauss'* 1794 *notebook* [**30**].

with tetrahedral parameters $e^{i\pi/3}$ and/or $e^{i\pi/2}$. Since the invariant trace field for cusped manifolds is generated by the tetrahedral parameters [**29**], the invariant trace fields are as given above.

We now address the commensurability of these links. In case (1), a direct computation in Snap [**17**] verifies that one such $M$ is arithmetic, namely the quotient of the square weave. Any link with fundamental domain consisting only of squares must be commensurable to this one. Since $M$ is cusped, has finite volume, is arithmetic, and has the same invariant trace field as the Whitehead link complement, $M$ is commensurable to the Whitehead link complement (see for example, [**23**, Theorem 8.2.3]).

For case (2), since $T_{\mathcal{L}}$ contains only triangles and hexagons, it uses tiles only of the type 3.6.3.6 or 3.3.6.6 by Lemma 3.3. As observed in [**20**, Section 1], by stacking horizontal strips made up of only one type of tile, we can obtain infinitely many biperiodic tilings; examples are shown in Figures 8 and 9 (left).

Moreover, in any biperiodic tiling with just triangles and hexagons, such a horizontal strip always exists, and translation along the strip is one of the directions of the biperiodic action. Each strip of the tiles 3.6.3.6 or 3.3.6.6 consists of strips of four types of parallelograms, each of which consists of half of the hexagon and a triangle, as shown in Figure 10. These four parallelograms are related by reflections and $\pi$-rotations. Since we are using only tiles of the type 3.6.3.6 or 3.3.6.6, we can construct the biperiodic tiling using just these four parallelograms. Because they are all related by reflections and $\pi$-rotations, this implies all such tilings are commensurable.

A direct computation in Snap [**17**] verifies that one of these links is arithmetic: namely the complement of the quotient of the triaxial link $M$ (see Figure 11). Since $M$ is cusped, has finite volume, is arithmetic, and has the same invariant trace field as the figure-8 knot complement, $M$ is commensurable to the figure-8 knot complement [**23**]. Hence, the commensurability claim follows for all biperiodic tilings containing only triangles and hexagons.

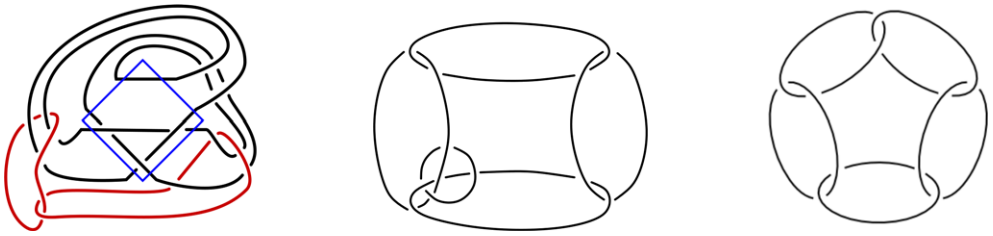

FIGURE 12 (colour online). *K* (*left and center*) *and minimally twisted* 5*-chain link* (*right*).

For case (3), let $\mathcal{L}_1$ and $\mathcal{L}_2$ be any two semi-regular links with no bigons, and at least one hexagon and one square per fundamental domain. By Theorem 3.5 (2), $\mathrm{vol}(L_1) = p_1\, v_{\mathrm{tet}} + q_1\, v_{\mathrm{oct}}$ and $\mathrm{vol}(L_2) = p_2\, v_{\mathrm{tet}} + q_2\, v_{\mathrm{oct}}$ for certain positive integers $p_1, q_1, p_2, q_2$.

If $\mathcal{L}_1$ and $\mathcal{L}_2$ are commensurable, then there exist integers $A$ and $B$ such that

$$A(p_1\, v_{\mathrm{tet}} + q_1\, v_{\mathrm{oct}}) = B(p_2\, v_{\mathrm{tet}} + q_2\, v_{\mathrm{oct}}) \Longrightarrow (A\, p_1 - B\, p_2)v_{\mathrm{tet}} = (B\, q_2 - A\, q_1)v_{\mathrm{oct}}.$$

Assuming $v_{\mathrm{tet}}$ and $v_{\mathrm{oct}}$ are rationally independent, this equation implies that

$$\frac{A}{B} = \frac{p_2}{p_1} \quad \text{and} \quad \frac{A}{B} = \frac{q_2}{q_1} \Longrightarrow p_1\, q_2 - q_1\, p_2 = 0.$$

By Theorem 3.4, there exist infinitely many semi-regular links $\mathcal{L}_i$ with no bigons, such that for any pair $\mathcal{L}_{i_1}$, $\mathcal{L}_{i_2}$,

$$p_{i_1}\, q_{i_2} - q_{i_1}\, p_{i_2} \neq 0.$$

Hence, these links $\mathcal{L}_i$ are pairwise incommensurable. □

Figure 9 (right) shows the tiling for $\mathcal{L}_2$, which is part of a family $\mathcal{L}_j$ with one hexagon and $4j$ squares per fundamental domain. All the semi-regular links $\mathcal{L}_j$ have the same invariant trace field.

## 5. *The triaxial link*

The triaxial link $\mathcal{L}$ is shown in Figure 11 with its projection, the trihexagonal tiling. It has long been used for weaving, and appears to have been considered mathematically by Gauss, who drew it in his 1794 notebook; see [**30**].

Let $L$ be the alternating quotient of the triaxial link in $T^2 \times I$. This can be described as a link $K$ in $S^3$ by drawing a fundamental domain on a Heegaard torus in $S^3$, then adding the Hopf link given by the cores of the two Heegaard tori, as in Figure 12 (left). After isotopy, the diagram of $K$ appears as in Figure 12 (center). This link complement is isometric to the complement of the minimally twisted 5-chain link, shown in Figure 12 (right), although the links are not isotopic: $K$ is the link $L12n2232$, and the minimally twisted 5-chain link is $L10n113$ in the Hoste–Thistlethwaite census of links up to 14 crossings [**21**]. Among its many interesting properties, $S^3 - K$ is conjectured to be the 5-cusped manifold with the smallest hyperbolic volume, and most of the hyperbolic manifolds in the cusped census can be obtained as its Dehn fillings [**24**].

For a semi-regular biperiodic alternating link, Theorem 3.5 provides a decomposition of the link complement into ideal hyperbolic torihedra. We say a torihedron is *right-angled* if it admits a hyperbolic structure in which all dihedral angles on edges equal $\pi/2$. In this section, we prove that only two semi-regular biperiodic alternating links admit a decomposition into right-angled torihedra: the square weave $\mathcal{W}$ studied in [**13**], and the triaxial link $\mathcal{L}$.

THEOREM 5.1. *The square weave $\mathcal{W}$ and the triaxial link $\mathcal{L}$ are the only semi-regular links such that right-angled torihedra give the complete hyperbolic structure. Thus, the links $\mathcal{W}$ and $\mathcal{L}$ have totally geodesic checkerboard surfaces.*

Theorem 5.1 implies that no semi-regular biperiodic alternating links have right-angled torihedra besides the square weave and the triaxial link. It is still unknown whether there are biperiodic alternating links that are not semi-regular with a right-angled torihedral decomposition.

QUESTION 5.2. Besides the square weave $\mathcal{W}$ and the triaxial link $\mathcal{L}$, do there exist any other right-angled biperiodic alternating links?

*Proof of Theorem* 5.1. First, we claim that if $\mathcal{L}$ has bigons, then the torihedra cannot be right-angled. For if there is a bigon, Lemma 2.5 implies that there is an edge of degree 6. If the torihedra were right-angled, the angle sum on this edge would be $(\pi/2) * 6 = 3\pi$, which is impossible. Thus $\mathcal{L}$ has no bigons, and all vertices of $T_{\mathcal{L}}$ are 4-valent.

By Theorem 3.5, there is a decomposition of any semi-regular alternating link into regular ideal bipyramids on the faces of $T_{\mathcal{L}}$. In this case, by Lemma 3.3, the only faces that occur are triangles, squares, and hexagons.

We obtain the torihedral decomposition from the bipyramid decomposition of Theorem 3.5 by first splitting each bipyramid into two pyramids, and then gluing vertical faces. Splitting into pyramids cuts in half the angle at the corresponding horizontal edge. Recall that a horizontal edge of a regular ideal bipyramid over an $n$-gon has angle $2\pi/n$ (see the proof of Lemma 3.7). Thus, splitting along a square gives angle $\pi/4$, splitting along a hexagon gives angle $\pi/6$. We already have two pyramids over triangular faces, which are regular ideal tetrahedra with angle $\pi/3$.

Now, when we glue along vertical faces, the angle coming from one side of the shared face is added to the angle coming from the other to give the new angle on the horizontal edge. There are six cases.

(1) A hexagon is adjacent to a hexagon. Then, the angle on the adjacent horizontal edge is $\pi/6 + \pi/6 = \pi/3$.
(2) A hexagon is adjacent to a triangle. The angle is $\pi/6 + \pi/3 = \pi/2$.
(3) A hexagon is adjacent to a square. The angle is $\pi/6 + \pi/4 = 5\pi/12$.
(4) A triangle is adjacent to a triangle. The angle is $\pi/3 + \pi/3 = 2\pi/3$.
(5) A triangle is adjacent to a square. The angle is $\pi/3 + \pi/4 = 7\pi/12$.
(6) A square is adjacent to a square. The angle is $\pi/4 + \pi/4 = \pi/2$.

Figure 13 shows the angles on horizontal edges of the torihedra for all five vertex types from Lemma 3.3. Note that the only cases that yield right angles are the edges where two adjacent squares meet and the edges where hexagons are adjacent to triangles. In order for the entire torihedron to be right-angled, these are the only face adjacencies possible. Then, the only possible vertex types from Lemma 3.3 are 3.6.3.6 and 4.4.4.4. These semi-regular links are exactly the triaxial link and the square weave, respectively.

Finally, note that if gluing geodesic ideal torihedra gives a complete hyperbolic structure, then the checkerboard surfaces inherit a pleating. That is, each surface is obtained by attaching totally geodesic polygonal faces, coming from the geodesic faces of the torihedra, joined along their edges at angles determined by the dihedral angles of the torihedra. The amount of bending, or pleating angle, is determined by the dihedral angles of the torihedra glued at that edge. In the case that the torihedra are right angled, then the pleating angle at each ideal edge will be $\pi/2 + \pi/2 = \pi$, or in other words the surface will be straight, not bent, at each edge. It follows that the surface is totally geodesic. □

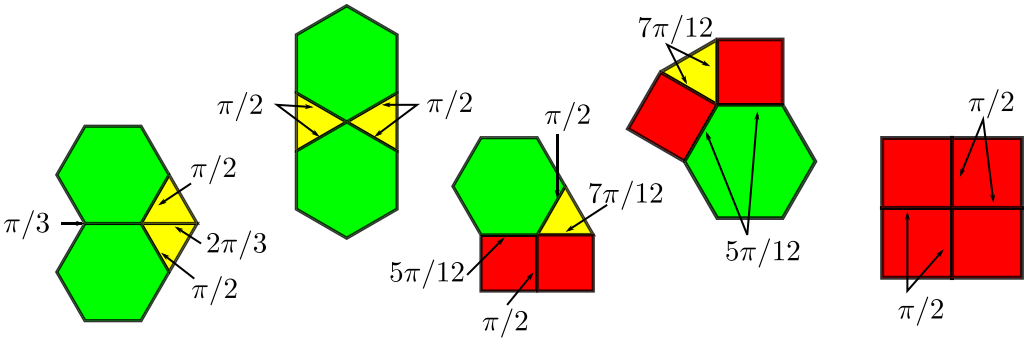


FIGURE 13 (colour online). *Angles on horizontal edges for the five vertex types.*

## 6. *Proof of the Volume Density Conjecture for the triaxial link*

In [10, 12, 13], we considered biperiodic alternating links as limits of sequences of finite hyperbolic links. We focused on the asymptotic behavior of two basic invariants, one geometric and one diagrammatic, for a hyperbolic link $K$: The *volume density* of $K$ is defined as $\mathrm{vol}(K)/c(K)$, and the *determinant density* of $K$ is defined as $2\pi \log \det(K)/c(K)$, where $c(K)$ denotes crossing number. The volume density is known to be bounded by the volume of the regular ideal octahedron, $v_{\mathrm{oct}} \approx 3.66386$, and the same upper bound is conjectured for the determinant density.

In [10], we defined the following notion of convergence of links, and proved that for any sequence of alternating links $K_n$ that converge to a biperiodic alternating link $\mathcal{L}$ in this sense, the determinant densities of $K_n$ converge to a type of determinant density of $\mathcal{L}$.

DEFINITION 6.1 [10, 13]. We will say that a sequence of alternating links $K_n$ *Følner converges almost everywhere* to the biperiodic alternating link $\mathcal{L}$, denoted by $K_n \xrightarrow{\mathrm{F}} \mathcal{L}$, if the respective projection graphs $\{G(K_n)\}$ and $G(\mathcal{L})$ satisfy the following: There are subgraphs $G_n \subset G(K_n)$ such that

(i) $G_n \subset G_{n+1}$, and $\bigcup G_n = G(\mathcal{L})$,
(ii) $\lim_{n\to\infty} |\partial G_n|/|G_n| = 0$, where $|\cdot|$ denotes number of vertices, and $\partial G_n \subset G(\mathcal{L})$ consists of the vertices of $G_n$ that share an edge in $G(\mathcal{L})$ with a vertex not in $G_n$,
(iii) $G_n \subset G(\mathcal{L}) \cap (n\Lambda)$, where $n\Lambda$ represents $n^2$ copies of the $\Lambda$-fundamental domain for the lattice $\Lambda$ such that $L = \mathcal{L}/\Lambda$,
(iv) $\lim_{n\to\infty} |G_n|/c(K_n) = 1$.

DEFINITION 6.2 (Definition 4.4 [13]). A diagram has *no cycle of tangles* if whenever a disk embedded in the torus meets the diagram transversely in exactly four edges, then the disk contains a single twist region; that is, a sequence of bigons or exactly one crossing.

As above, let $\mathcal{W}$ be the infinite square weave. Using the right-angled hyperbolic structure of $\mathcal{W}$ in an essential way, in [13] we proved:

THEOREM 6.3 [13]. *Let $K_n$ be any alternating hyperbolic link diagrams with no cycles of tangles such that $K_n \xrightarrow{\mathrm{F}} \mathcal{W}$. Then for $K_n$, the volume and determinant densities satisfy:*

$$\lim_{n\to\infty} \frac{\mathrm{vol}(K_n)}{c(K_n)} = \lim_{n\to\infty} \frac{2\pi \log \det(K_n)}{c(K_n)} = v_{\mathrm{oct}}.$$

The volume density of a biperiodic alternating link is defined as $\mathrm{vol}((T^2 \times I) - L)/c(L)$, where $c(L)$ is the crossing number of the reduced alternating projection of $L$ on the torus, which is minimal. Hence, as $K_n \xrightarrow{\mathrm{F}} \mathcal{W}$, the volume densities of $K_n$ converge to the volume density of $\mathcal{W}$, which is $v_{\mathrm{oct}}$; see [13].

For determinant density, there is a toroidal invariant of $\mathcal{W}$ that appears as the limit of the determinant density, namely the Mahler measure of the two-variable characteristic polynomial of the toroidal dimer model on an associated biperiodic graph, which measures the entropy of the dimer model. In [10], this diagrammatic result for $\mathcal{W}$ was extended to *any* biperiodic alternating link $\mathcal{L}$:

THEOREM 6.4 [10]. *Let $\mathcal{L}$ be any biperiodic alternating link, with alternating quotient link $L$. Let $p(z, w)$ be the characteristic polynomial of the associated toroidal dimer model. Then,*

$$K_n \xrightarrow{\mathrm{F}} \mathcal{L} \Longrightarrow \lim_{n\to\infty} \frac{\log \det(K_n)}{c(K_n)} = \frac{m(p(z,w))}{c(L)}.$$

The following conjectures are motivated by Theorems 6.3 and 6.4:

CONJECTURE 6.5 (Volume Density Conjecture). Let $\mathcal{L}$ be any biperiodic alternating link, with alternating quotient link $L$. Let $K_n$ be alternating hyperbolic links such that $K_n \xrightarrow{\mathrm{F}} \mathcal{L}$. Then,

$$\lim_{n\to\infty} \frac{\mathrm{vol}(K_n)}{c(K_n)} = \frac{\mathrm{vol}((T^2 \times I) - L)}{c(L)}$$

CONJECTURE 6.6 (Toroidal Vol-Det Conjecture). Let $\mathcal{L}$ be any biperiodic alternating link, with alternating quotient link $L$. Let $K_n$ be alternating hyperbolic links such that $K_n \xrightarrow{\mathrm{F}} \mathcal{L}$. Then,

$$\mathrm{vol}((T^2 \times I) - L) \leqslant 2\pi\, m(p(z,w)).$$

The Toroidal Vol-Det Conjecture is studied in more detail in forthcoming work [11].

Theorem 6.3 proves both conjectures with equality for the square weave $\mathcal{W}$. In Theorem 6.7, we establish both conjectures with equality for the triaxial link as well. By Theorem 5.1, these are the only semi-regular links such that right-angled torihedra give the complete hyperbolic structure.

THEOREM 6.7. *Let $\mathcal{L}$ be the triaxial link. Let $K_n$ be any alternating hyperbolic link diagrams with no cycles of tangles such that $K_n \xrightarrow{\mathrm{F}} \mathcal{L}$. Then,*

$$\lim_{n\to\infty} \frac{\mathrm{vol}(K_n)}{c(K_n)} = \lim_{n\to\infty} \frac{2\pi \log \det(K_n)}{c(K_n)} = \frac{\mathrm{vol}((T^2 \times I) - L)}{c(L)} = \frac{10\, v_{\mathrm{tet}}}{3}.$$

*Proof.* By Theorem 3.5,

$$\frac{\mathrm{vol}((T^2 \times I) - L)}{c(L)} = \frac{10\, v_{\mathrm{tet}}}{3}.$$

By [10, Example 4.2],

$$\lim_{n\to\infty} \frac{2\pi \log \det(K_n)}{c(K_n)} = \frac{2\pi\, m(p(z,w))}{c(L)} = \frac{10\, v_{\mathrm{tet}}}{3}.$$

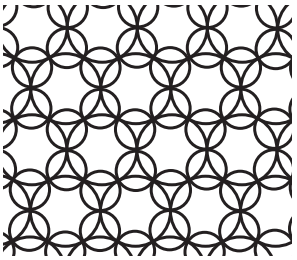

FIGURE 14. *Circle pattern for $P(\mathcal{L})$ for the triaxial link $\mathcal{L}$.*

It remains to prove Conjecture 6.5 for the triaxial link $\mathcal{L}$. Namely,

$$K_n \xrightarrow{\mathrm{F}} \mathcal{L} \Longrightarrow \lim_{n\to\infty} \frac{\mathrm{vol}(K_n)}{c(K_n)} = \frac{\mathrm{vol}((T^2 \times I) - L)}{c(L)}.$$

We adapt the proof of [**13**, Theorem 1.4], which proves Conjecture 6.5 for $\mathcal{W}$.

By Theorem 5.1, the checkerboard surfaces of $\mathcal{L}$ are totally geodesic, with the faces of the torihedra lifting to totally geodesic hyperplanes in the universal cover $\mathbb{H}^3$ of $\mathbb{R}^3 - \mathcal{L}$, meeting at right angles. This forces these hyperplanes to meet $\partial\mathbb{H}^3 = \widehat{\mathbb{C}}$ in the circle pattern shown in Figure 14.

Now proceed as in [**13**]. If $K_n \subset S^3$ is a sequence of alternating hyperbolic links such that $K_n \xrightarrow{\mathrm{F}} \mathcal{L}$, then by [**13**, Theorem 4.13] the volumes of $K_n$ are bounded below by twice the volume of the polyhedron obtained from the checkerboard polyhedron of $K_n$ by assigning right angles to all the edges. Denote this by $P_n$.

Now we repeat the proof of [**13**, Lemma 5.3], replacing the disk pattern coming from $\mathcal{W}$ with that of Figure 14 coming from $\mathcal{L}$. In that proof, each instance of $v_{\mathrm{oct}}$ (the volume density of $\mathcal{W}$) must be replaced by $(10v_{\mathrm{tet}}/3)$, the volume density of $\mathcal{L}$.

Finally, step through the proof of Theorem 1.4 in [**13**, section 5]. Again, first check that the hypotheses are satisfied for the lemma analogous to [**13**, Lemma 5.3] (with $v_{\mathrm{oct}}$ replaced by $10v_{\mathrm{tet}}/3$). Note for condition (2), the argument is the same but the constant 4 is replaced by 6 (this does not affect the limit). For (1), $|\partial B(x,\ell)| = 6\ell$. Otherwise, the argument is identical. Then, this lemma and [**13**, Theorem 4.13] imply

$$\lim_{n\to\infty} \frac{\mathrm{vol}(K_n)}{c(K_n)} = \frac{10v_{\mathrm{tet}}}{3}. \qquad \square$$

## 7. *Hyperbolicity for alternating links in $T^2 \times I$*

In this section, we generalize the results on hyperbolicity and triangulations to wider classes of links on $T^2 \times I$. We prove that if a link $L$ in $T^2 \times I$ admits a certain kind of alternating diagram on the torus, then $(T^2 \times I) - L$ is hyperbolic. Moreover, for a (possibly incomplete) hyperbolic structure on the complement, we find a triangulation that satisfies Thurston's gluing equations. We show that this triangulation is positively oriented and unimodular. This leads to lower and upper bounds on the hyperbolic volume of $(T^2 \times I) - L$, denoted by $\mathrm{vol}(L)$.

To describe the links, we need a few definitions. First, the definition of connected sums of knots in $S^3$ can be extended to knots in $T^2 \times I$. We are concerned with knots with reduced diagrams that are not connected sums, as in the following definition.

DEFINITION 7.1. A diagram is *weakly prime* if whenever a disk embedded in the diagram surface meets the diagram transversely in exactly two edges, then the disk contains a simple edge of the diagram and no crossings.

In addition, we will also need Definition 6.2 and the following:

DEFINITION 7.2. A geodesic ideal triangulation satisfying the edge gluing equations is called *unimodular* if every tetrahedron has an edge parameter $z$ that satisfies $|z| = 1$.

By equation (7.1), a tetrahedron is unimodular if and only if its vertex link triangles are isosceles.

DEFINITION 7.3. Let $B_n$ denote the hyperbolic regular ideal bipyramid whose link polygons at the two coning vertices are regular $n$-gons. For a face $f$ of $G(L)$, let $|f|$ denote the degree of the face. Let $L$ be a link in $T^2 \times I$ with an alternating diagram on $T^2 \times \{0\}$, and let $T_L$ be the toroidal graph defined in Lemma 2.5. Define the *bipyramid volume* of $L$ as

$$\mathrm{vol}^{\Diamond}(L) = \sum_{f \in \{\text{faces of } T_L\}} \mathrm{vol}(B_{|f|}).$$

Note that for all semi-regular links, Theorem 3.5 implies $\mathrm{vol}(L) = \mathrm{vol}^{\Diamond}(L)$.

DEFINITION 7.4. Let $L$ be a link in $T^2 \times I$ with an alternating diagram on $T^2 \times \{0\}$, and let $P(L)$ be the torihedron as in Theorem 2.2. Assume that $P(L)$ admits an ideal right-angled hyperbolic structure. Define the *right-angled volume* of $L$ as

$$\mathrm{vol}^{\perp}(L) = 2\mathrm{vol}(P(L)).$$

Note that for the square weave and triaxial link, Theorem 5.1 implies $\mathrm{vol}(L) = \mathrm{vol}^{\perp}(L)$.

Suppose that $K$ is a link in $S^3$ with a prime, alternating, twist-reduced diagram with no cycle of tangles, and with bigons removed. In [**13**, Theorem 4.13], we proved that the two checkerboard polyhedra coming from $K$, when given an ideal hyperbolic structure with all right angles, have volume providing a lower bound for $\mathrm{vol}(S^3 - K)$.

In Theorem 7.5, we extend [**13**, Theorem 4.13] to any link in $T^2 \times I$ satisfying similar conditions. The methods involved in proving Theorem 7.5 are different from those used in [**13**], which relied on volume bounds via guts of 3-manifolds cut along essential surfaces. Here, the proof of Theorem 7.5 involves circle packings, geometric structures on triangulations, and the convexity of volume.

THEOREM 7.5. *Let $L$ be a link in $T^2 \times I$ with a weakly prime alternating diagram on $T^2 \times \{0\}$ with no bigons. If $L$ has no cycle of tangles, then*

(1) *$(T^2 \times I) - L$ is hyperbolic;*
(2) *$(T^2 \times I) - L$ admits a (possibly incomplete) hyperbolic structure obtained from an ideal, positively oriented, unimodular triangulation;*
(3) *under the structure of item (2), the torihedron $P(L)$ is right-angled;*
(4) $\mathrm{vol}^{\perp}(L) \leqslant \mathrm{vol}(L) \leqslant \mathrm{vol}^{\Diamond}(L)$.

Note that by Theorems 3.5 and 5.1, both inequalities in (4) become equalities for the square weave and the triaxial link: all three give the volume of the complete structure. Thus, both upper and lower bounds of Theorem 7.5, (4) are sharp. In general, the bounds in (4) are volumes of incomplete ideal hyperbolic structures on $(T^2 \times I) - L$.

REMARK 7.6. Theorem 7.5 should be compared to the results of [**22**]. That paper also implies that the links in Theorem 7.5 are hyperbolic, and gives a lower bound on volume in terms of the number of twist regions of the diagram. Since the diagram here has no bigons, this

also amounts to a lower volume bound in terms of the crossing number. However, the results of Theorem 7.5 are stronger in this case because they give an explicit hyperbolic structure, although that structure is likely incomplete. Moreover, the volume bound of Theorem 7.5 is known to be sharp for the square weave and triaxial link.

The proof of Theorem 7.5 will proceed in the order (3), (2), (1), (4). The proof relies on a fundamental result about the existence of certain circle patterns on the torus, due to Bobenko and Springborn [8]. The following special case of [8, Theorem 4] applies.

THEOREM 7.7 [8]. *Suppose that $G$ is a 4-valent graph on the torus $T^2$, and $\theta \in (0, 2\pi)^E$ is a function on edges of $G$ that sums to $2\pi$ around each vertex. Let $G^*$ denote the dual graph of $G$. Then, there exists a circle pattern on $T^2$ with circles circumscribing faces of $G$(after isotopy of $G$) and having exterior intersection angles $\theta$, if and only if the following condition is satisfied:*

> *Suppose that we cut the torus along a subset of edges of $G^*$, obtaining one or more pieces. For any piece that is a disk, the sum of $\theta$ over the edges in its boundary must be at least $2\pi$, with equality if and only if the piece consists of only one face of $G^*$ (only one vertex of $G$).*

*The circle pattern on the torus is uniquely determined up to similarity.*

*Proof of Theorem* 7.5. For $L$ as stated, let $G(L)$ be its projection graph on $T^2 \times \{0\}$, and let $\theta(e) = \pi/2$ for every edge $e$ in $G(L)$. For this choice of angles, we now verify the condition of Theorem 7.7. This will prove the existence of an orthogonally intersecting circle pattern that is combinatorially equivalent to $G(L)$.

Let $C$ be a simple closed curve in $T^2 \times \{0\}$ that intersects $n$ edges of $G(L)$ transversely, and bounds a disk in $T^2 \times \{0\}$. Since $G(L)$ is weakly prime, $n \geqslant 3$. If $n \geqslant 5$, the angle sum is greater than $2\pi$. Hence, it remains only to check the cases $n = 3$ and $n = 4$.

The curve $C$ bounds a disk $D$. Let $V_I$ denote the number of vertices of $G(L)$ that lie in $D$, and let $E_I$ denote the number of edges of $G(L)$ inside $D$ disjoint from $C$. Because $G(L)$ is 4-valent, $n + 2E_I = 4V_I$ . It follows that $n$ is even, ruling out $n = 3$.

So, suppose $n = 4$. In this case, the angle sum equals $2\pi$. Hence, the condition of Theorem 7.7 is satisfied if and only if the disk bounded by $C$ contains exactly one crossing. Since $G(L)$ has no bigons, this condition is equivalent to the condition that $L$ has no cycle of tangles, which holds by hypothesis. Thus, Theorem 7.7 applies.

Therefore, there exists an orthogonal circle pattern on the torus with circles circumscribing the faces of $G(L)$. Lifting this circle pattern to the universal cover of the torus defines an orthogonal biperiodic circle pattern on the plane. Considered as the plane at infinity for $\mathbb{H}^3$, this circle pattern defines a right-angled biperiodic ideal hyperbolic polyhedron in $\mathbb{H}^3$. The torihedron $P(L)$ is its toroidal quotient, which is realized as an ideal right-angled hyperbolic torihedron, as required for Theorem 7.5 part (3).

Now, let $\mathcal{T}$ be the stellated bipyramid triangulation. The right-angled structure can be used to assign shape parameters in $\mathbb{C}$ to the tetrahedra of $\mathcal{T}$. In particular, let $G_L^c$ be the central triangulation of $G(L)$, given by adding a central vertex in each face and edges in each face to triangulate the faces; see Figure 15. Since the condition of Theorem 7.7 holds, each face of $G(L)$ is inscribed in a geometric circle, such that the center of the circle lies in the interior of the face. Thus, we may take the center of the circle to be the central vertex of $G_L^c$. Therefore, every triangle of $G_L^c$ is isosceles, with the two equal edges coming from $G_L^c - E(G(L))$. When the isosceles triangles are paired, they form right-angled kites, which is the quad graph of the orthogonal circle pattern.

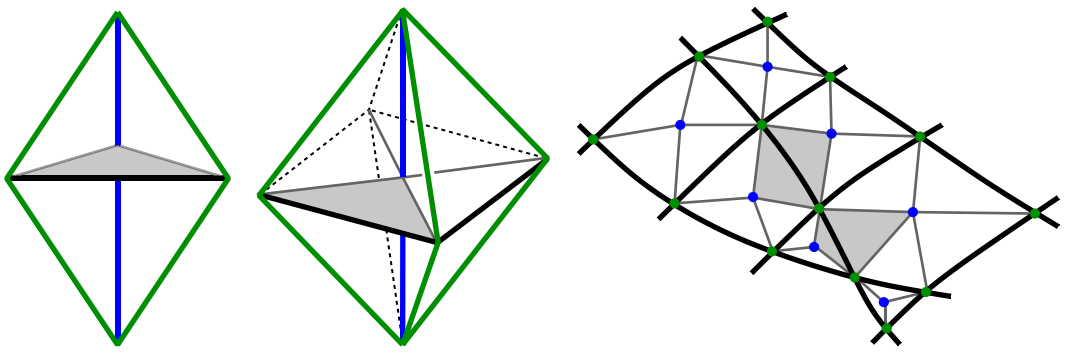


FIGURE 15 (colour online). (a) *A tetrahedron in $\mathcal{T}$ with stellating (blue), vertical (green), and horizontal (black) edges. A link triangle for an ideal vertex at $\infty$ is shaded.* (b) *Tetrahedra are glued at the stellating edge, centrally triangulating faces of $G(L)$ on $T^2 \times \{0\}$.* (c) *Graphs $G(L)$ (black) and $G_L^c$ (gray and black). Shaded triangles indicate the four tetrahedra glued along one horizontal edge.*

Each triangle of $G_L^c$ corresponds to a unique tetrahedron in $\mathcal{T}$. We assign edge parameters to a tetrahedron of $\mathcal{T}$ as follows. Recall that for an ideal hyperbolic tetrahedron, a *vertex link triangle* is the boundary of a horoball neighborhood of an ideal vertex. We view the triangles of $G_L^c$ as vertex link triangles for $\mathcal{T}$. If the angles of the link triangle are $\alpha$, $\beta$, $\gamma$ in clockwise order, then the edge parameter of the edge with dihedral angle $\alpha$ is given by

$$z(\alpha) = e^{i\alpha} \sin(\gamma)/\sin(\beta). \tag{7.1}$$

This assigns edge parameters to tetrahedra in $\mathcal{T}$.

Since every angle of every triangle is in $(0, \pi)$, every edge parameter has positive imaginary part; that is, all the tetrahedra are positively oriented. Moreover, because every triangular face of $G_L^c$ is isosceles, with the congruent angles adjacent to the edges of $G(L)$, equation (7.1) implies that the edge parameter at the stellating edge of every tetrahedron in $\mathcal{T}$ equals $e^{i\alpha}$ for some $\alpha$. Since every tetrahedron has an edge parameter which lies on the unit circle, the ideal triangulation is unimodular.

To show the ideal tetrahedra with these edge parameters give a (possibly incomplete) hyperbolic structure on $(T^2 \times I) - L$, we will show that the edge gluing equations are satisfied for each of the three types of edges (stellating, vertical and horizontal).

First, note that the angle sum around a stellating edge is $2\pi$ because of the planar embedding of $G_L^c$. If the angles are $\alpha_1, \ldots, \alpha_k$, then the corresponding edge gluing equation is $e^{i\alpha_1} \ldots e^{i\alpha_k} = 1$. Hence, the edge gluing equations are satisfied at the stellating edges.

At a vertical edge, the planar embedding again implies that the angle sum is $2\pi$, satisfying the rotational part of the edge gluing equation. Because the triangles of the graph $G_L^c$ around a vertex of $G(L)$ are exactly the vertex link triangles of the ideal tetrahedra adjacent to the vertical edge, the tetrahedra glue without translation along the edge, hence rotational and translational parts of the equation are both satisfied.

Since $L$ has no bigons, the horizontal edges of $\mathcal{T}$ are identified in pairs that share a common vertex on the torihedron $P(L)$ (see Figure 1). Hence, there are four tetrahedra whose horizontal edges are identified to one edge in $\mathcal{T}$. For each tetrahedron in $\mathcal{T}$, each horizontal edge is opposite to the stellating edge, so it has the same edge parameter $e^{i\alpha}$ and thus is unimodular.

For the four tetrahedra whose horizontal edges are identified, their link triangles glue along the horizontal edges to form two right-angled kites, whose diagonals are these edges. See

Figure 15. The dihedral angle at the horizontal edge equals the corresponding vertex angle of the kite. Since every kite is right-angled, its non-congruent vertex angles sum to $\pi$. So for each horizontal edge, the angle contribution from these four tetrahedra is $2\pi$.

Now, because the horizontal edge parameters are unimodular, these edge parameters multiply to 1. Therefore, the edge parameters at the horizontal edges satisfy the edge gluing equations. This completes the proofs of Theorem 7.5 parts (2) and (3).

A positively oriented geometric triangulation implies part (1); see for example [16].

To prove the lower bound, we use the lower volume bound given by the volume of a representation. Because $(T^2 \times I) - L$ admits a hyperbolic structure, it admits a representation of the fundamental group into $\mathrm{PSL}(2, \mathbb{C})$. The volume of this representation is $2\,\mathrm{vol}(P(L))$. Francaviglia showed that the volume of such a representation gives a lower bound on the volume of the complete structure [18]. The lower bound in part (4) follows.

Finally, the tetrahedra in $\mathcal{T}$ combine along every stellating edge to give a hyperbolic ideal bipyramid over a face of $T_L$. The upper bound in part (4) follows from the fact that the maximal volume of a complete ideal $n$–bipyramid is obtained uniquely by the regular $n$–bipyramid [1, Theorem 2.1].

This completes the proof of Theorem 7.5. □

*Acknowledgements.* We thank Colin Adams for useful discussions, and note that part (1) of Theorem 3.5 was proved independently in [3]. We thank the organizers of the workshops *Interactions between topological recursion, modularity, quantum invariants and low-dimensional topology* at MATRIX and *Low-dimensional topology and number theory* at MFO (Oberwolfach), where part of this work was done. We thank Tom Ruen, whose figures at [33] were very helpful for this project.

## *References*

**1.** C. Adams, 'Bipyramids and bounds on volumes of hyperbolic links', *Topology Appl.* 222 (2017) 100–114.
**2.** C. Adams, H. Bennett, C. Davis, M. Jennings, J. Kloke, N. Perry and E. Schoenfeld, 'Totally geodesic Seifert surfaces in hyperbolic knot and link complements. II', *J. Differential Geom.* 79 (2008) 1–23.
**3.** C. Adams, A. Calderon and N. Mayer, 'Generalized bipyramids and hyperbolic volumes of alternating $k$–uniform tiling links', Preprint, 2017, arXiv:1709.00432 [math.GT].
**4.** C. Adams and G. Kehne, 'Bipyramid decompositions of multi-crossing link complements', Preprint, 2016, arXiv:1610.03830 [math.GT].
**5.** C. Adams and E. Schoenfeld, 'Totally geodesic Seifert surfaces in hyperbolic knot and link complements. I', *Geom. Dedicata* 116 (2005) 237–247.
**6.** I. R. Aitchison, E. Lumsden and J. H. Rubinstein, 'Cusp structures of alternating links', *Invent. Math.* 109 (1992) 473–494.
**7.** I. Aitchison and L. Reeves, 'On archimedean link complements', *J. Knot Theory Ramifications* 11 (2002) 833–868.
**8.** A. I. Bobenko and B. A. Springborn, 'Variational principles for circle patterns and Koebe's theorem', *Trans. Amer. Math. Soc.* 356 (2004) 659–689.
**9.** A. Bogdanov, V. Meshkov, A. Omelchenko and M. Petrov, 'Classification of textile links', 2007, https://www.researchgate.net/publication/267397986_CLASSIFICATION_OF_TEXTILE_LINKS.
**10.** A. Champanerkar and I. Kofman, 'Determinant density and biperiodic alternating links', *New York J. Math.* 22 (2016) 891–906.
**11.** A. Champanerkar, I. Kofman and M. Lalin, 'Mahler measure and the vol-det conjecture', *J. Lond. Math. Soc.*, to appear.
**12.** A. Champanerkar, I. Kofman and J. S. Purcell, 'Density spectra for knots', *J. Knot Theory Ramifications* 25 (2016) 1640001, 11.
**13.** A. Champanerkar, I. Kofman and J. S. Purcell, 'Geometrically and diagrammatically maximal knots', *J. Lond. Math. Soc.* (2) 94 (2016) 883–908.
**14.** A. Champanerkar, I. Kofman and J. S. Purcell, 'Volume bounds for weaving knots', *Algebr. Geom. Topol.* 16 (2016) 3301–3323.
**15.** E. Chesebro and J. DeBlois, 'Algebraic invariants, mutation and commensurability of link complements', *Pacific J. Math.* 267 (2014) 341–398.
**16.** Y.-E. Choi, 'Positively oriented ideal triangulations on hyperbolic three-manifolds', *Topology* 43 (2004) 1345–1371.

**17.** D. Coulson, O. A. Goodman, C. D. Hodgson and W. D. Neumann, 'Computing arithmetic invariants of 3-manifolds', *Experiment. Math.* 9 (2000) 127–152.
**18.** S. Francaviglia, 'Hyperbolic volume of representations of fundamental groups of cusped 3-manifolds', *Int. Math. Res. Not.* (2004) 425–459.
**19.** D. Futer and F. Guéritaud, 'From angled triangulations to hyperbolic structures', *Interactions between hyperbolic geometry, quantum topology and number theory*, Contemporary Mathematics 541 (eds A. Champanerkar, O. Dasbach, E. Kalfagianni, I. Kofman, W. Neumann and N. Stoltzfus; American Mathematical Society, Providence, RI, 2011) 159–182.
**20.** B. Grünbaum and G. C. Shephard, 'Tilings by regular polygons. Patterns in the plane from Kepler to the present, including recent results and unsolved problems', *Math. Mag.* 50 (1977) 227–247.
**21.** J. Hoste, 'The enumeration and classification of knots and links', *Handbook of knot theory* (Elsevier, Amsterdam, 2005) 209–232.
**22.** J. A. Howie and J. S. Purcell, 'Geometry of alternating links on surfaces', Preprint, 2017, arXiv:1712.01373.
**23.** C. Maclachlan and A. W. Reid, *The arithmetic of hyperbolic* 3*-manifolds*, Graduate Texts in Mathematics 219 (Springer, New York, 2003).
**24.** B. Martelli, C. Petronio and F. Roukema, 'Exceptional Dehn surgery on the minimally twisted five-chain link', *Comm. Anal. Geom.* 22 (2014) 689–735.
**25.** W. W. Menasco, 'Polyhedra representation of link complements', *Low-dimensional topology*, Contemporary Mathematics 20 (American Mathematical Society, Providence, RI, 1983) 305–325.
**26.** W. Menasco, 'Closed incompressible surfaces in alternating knot and link complements', *Topology* 23 (1984) 37–44.
**27.** J. Milnor, 'Hyperbolic geometry: the first 150 years', *Bull. Amer. Math. Soc. (N.S.)* 6 (1982) 9–24.
**28.** H. R. Morton and S. Grishanov, 'Doubly periodic textile structures', *J. Knot Theory Ramifications* 18 (2009) 1597–1622.
**29.** W. D. Neumann and A. W. Reid, 'Arithmetic of hyperbolic manifolds', *Topology '90*, Ohio State University Mathematical Research Institution Publications 1 (eds B. Apanasov, W. D. Neumann, A. W. Reid and L. Siebermann; de Gruyter, Berlin, 1992) 273–310.
**30.** J. H. Przytycki, 'From 3-moves to Lagrangian tangles and cubic skein modules', *Advances in topological quantum field theory*, NATO Science Series 179 (ed. J. M. Bryden; Kluwer Academic Publishers, Dordrecht, 2004) 71–125.
**31.** I. Rivin, 'Euclidean structures on simplicial surfaces and hyperbolic volume', *Ann. of Math.* (2) 139 (1994) 553–580.
**32.** W. P. Thurston, 'The geometry and topology of three-manifolds', Princeton University, 1979, http://www.msri.org/publications/books/gt3m/.
**33.** Wikipedia, 'Euclidean tilings by convex regular polygons', https://en.wikipedia.org/wiki/Euclidean_tilings_by_convex_regular_polygons. Figures by Tom Ruen http://en.wikipedia.org/wiki/User:Tomruen.

*Abhijit Champanerkar and Ilya Kofman*
*Department of Mathematics*
*College of Staten Island & The Graduate Center*
*City University of New York*
*New York, NY 10314*
*USA*

abhijit@math.csi.cuny.edu
ikofman@math.csi.cuny.edu

*Jessica S. Purcell*
*School of Mathematical Sciences*
*Monash University*
*9 Rainforest Walk, Victoria 3800*
*Australia*

jessica.purcell@monash.edu